

Modelling convective and radiative heat transfer in a glass melting model crucible

D. Cepite, A. Jakovics, B. Halbedel

Abstract

Numerical modelling of thermally and electromagnetically driven semi-transparent glass melt flow in an experimental model crucible has been done using both constant and temperature dependent physical properties of the melt. Impact of heat conduction, thermal and EM convection as well as radiation heat transfer has been analysed. Influence of absorption coefficient on the maximal temperature T_{\max} and temperature range ΔT in the melt has been estimated. Minimums in dependencies of T_{\max} and ΔT on absorption coefficient have been perceived. In case of temperature dependent physical properties corresponding to a real glass composition importance of the radiative heat transfer in reducing the risk of overheating the melt has been illustrated.

Introduction

Non-contact methods for stirring of glass melts are important to enhance homogeneity without inserting impurities into the melt. It is relevant for usage in manufacturing process of high quality glass products - optical lenses, pharmaceutical packaging etc.

In [1] implementation of Lorentz force created by interaction of the external magnetic field (in z direction Fig. 1) and electrical current flowing in the melt between the electrodes has been examined as a potential method for improving temperature homogeneity of the glass melt. In present study, main attention has been paid to influence of the radiation heat transfer on temperature distribution of the glass melt.

1. General Information

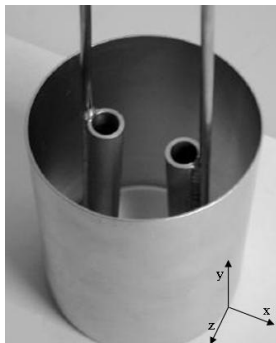


Fig. 1. Photograph of the model crucible

Numerical results model situation in a well conducting, glass melting model crucible 8 cm in diameter and 8 cm in height. Thermal energy is supplied to the system by Joule heat source originating from alternating electrical current with frequency 50 Hz flowing between two rod electrodes immersed in the melt 6 cm deep. In order to enhance more efficient mixing of the melt the crucible is inserted in the thermally isolated furnace placed in the air gap of an electromagnet system, which generates magnetic induction \mathbf{B} with the same frequency and effective value of $B=0.044$ T. In this situation Lorentz force is created due to interaction of homogeneous external alternating magnetic field with induction in z direction (Fig. 1) and alternating electrical current flowing in the melt. EM calculations in ANSYS as well as analysis of non-dimensional

frequency of the system [2] assure that induction effects are negligible and current and magnetic field does not influence each other.

2. Description of the mathematical model

2.1. Assumptions and boundary conditions

Mathematical background of the coupling among the EM, hydrodynamic and heat transfer processes has been discussed in detail in [1]. Temperature dependent physical properties of the melt have been used, for example, electrical conductivity $\sigma(T)=A_\sigma \cdot \exp(-B_\sigma/T)$, dynamic viscosity $\eta(T)=A_\eta \cdot \exp(-1/(B_\eta \cdot T^2 + C_\eta \cdot T + D_\eta))$, where A_i , B_i , C_i , D_i are approximation constants of experimentally estimated dependencies. The main assumptions of the model are:

- the flow of the melt is laminar. Typical Reynolds number $Re < 10$;
- in case of radiation heat exchange diffuse reflection on all boundaries has been assumed; media has been assumed grey and non-scattering;
- surfaces of the electrodes are assumed equipotent. Potentials φ_1 and $-\varphi_1$ have been set on the surfaces of the electrodes and zero potential on the side and bottom wall of the melt;
- the Lorentz force distribution is calculated in non-inductive approximation. Typical non-dimensional frequency for the melt in the model furnace $\hat{\omega} = 2\pi f \sigma_{melt} \mu_0 r_0^2 \ll 1$, where r_0 is a characteristic size of the system (radius of the crucible) and f is field's frequency. Additional calculations in ANSYS verify that potential change in electrodes is negligible due to the high ratio of conductivities ($\sigma_{electrodes}/\sigma_{melt} \approx 10^5$) and assumptions of equipotent surfaces and non-inductive approximation are well grounded. Fig. 2 illustrates the main boundary conditions of the mathematical model. Symmetric part, which is one-half of the full system, has been calculated. In case radiation heat transfer is not included, solution in one-fourth part of the system has been obtained.

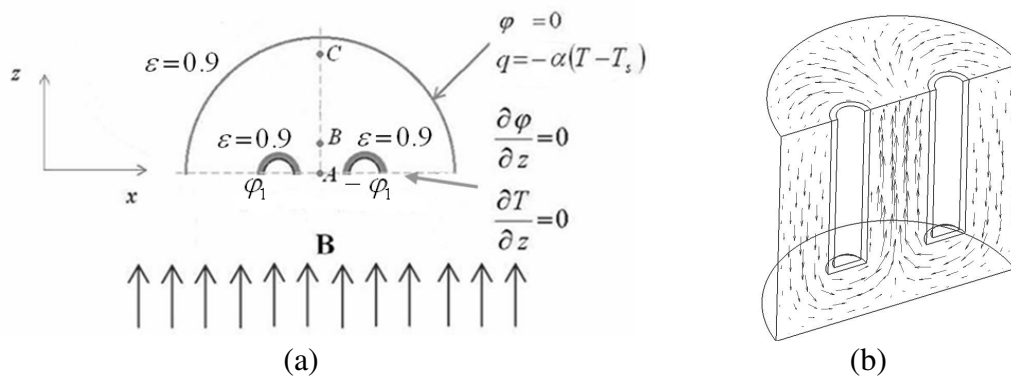


Fig. 2. Sketch of the model (view from the top - the melt with the two immersed hollow platinum electrodes) and boundary conditions (a); An example of velocity field caused by thermal and EM convection, $v_{max} \approx 1$ cm/s (in case Lorentz force is upwards oriented in the central part of the melt) (b)

2.2. Numerical implementation

Tetrahedral mesh for the 3D glass melt and hexahedral mesh for the electrodes with $3 \cdot 10^5$ elements (in total) is used. For the results presented in section 3.2. the mesh with $9 \cdot 10^5$ elements (in total) has been used. Steady state solutions are analysed. Maximal residual below $3 \cdot 10^{-5}$ and all imbalances below 1 % are used as a criteria for convergence of the model.

Hydrodynamics and heat transfer problems have been implemented in ANSYS CFX automatically, but EM is added by adapting the transport equation to be able to solve continuity equation for the electrical current \mathbf{j} . Radiation model P1 built in ANSYS CFX has

been used for radiation heat transfer calculation in semi-transparent glass. In case of analysis of absorption coefficient impact on temperature distribution Discrete transfer radiation model has been implemented for optically thin melt and Rosseland radiation heat transfer model for cases with optical thickness greater than 5 [3].

3. Results

3.1. Melt with temperature dependant physical properties

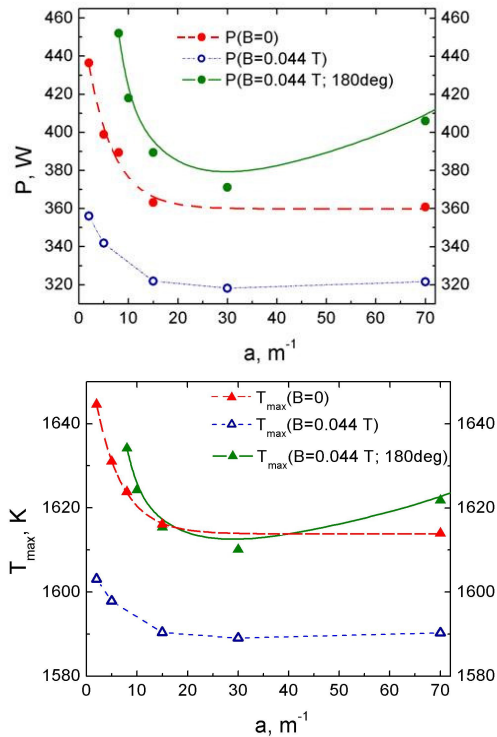


Fig. 3. Dependencies of total Joule heat production rate (a) and the maximal temperature (b) on absorption coefficient in case of B=0, upwards and down wards oriented Lorentz force in the central part of the melt ($U_{\text{eff}}=20$ V, $\alpha=180$ W/m²·K, $T_s=1545$ K according to Fig. 2)

of the melt due to 0° phase shift between AC and external magnetic field; in case B=0 as well.

In order to exclude the effect of non-linear temperature dependence of the physical properties of the melt, which may be the reason of increase of P and T_{max} in case absorption decreases (in optically thin absorption range), further study with constant physical properties of the melt has been done.

3.2. Melt with constant physical properties

Melt with the fixed physical properties (corresponding to properties of the semi-transparent melt in case of the fixed temperature 1640 K) has been used for analysing the influence of conduction, thermal and EM convection and radiation on temperature distribution.

Modelling results with and without radiation heat transfer have been compared in [4]. Numerical results show that there is the higher maximal temperature and temperature range and larger Joule heat production rate (for a fixed U_{eff} and thermal boundary conditions) in opaque than in semi-transparent melt with absorption coefficient $a=70$ m⁻¹. In order to generalize influence of semi-transparency on temperature distribution of the melt numerical experiments with different absorption coefficients have been done. In Fig. 3 dependence of total Joule heat production rate and maximal temperature on absorption coefficient have been shown. P1 radiation heat transfer model has been used in calculations. In case of Lorentz force suppressing the flow of the melt (180° phase shift between alternating current and the external magnetic field, which results in down wards oriented Lorentz force in the central part of the melt) the minimums arise in dependencies T_{max} and P versus absorption. T_{max} and P increase when absorption $a=30$ m⁻¹ decreases towards the values corresponding to optically thin media; it increases when absorption is increased from $a=30$ m⁻¹ to $a=70$ m⁻¹. T_{max} has been larger in case of opaque melt than in semi-transparent melt with $a=70$ m⁻¹. Therefore, the minimum should be expected in the rest of situations: in case of upwards oriented Lorentz force in the central part

The upper row in Fig. 4 corresponds to situation in opaque melt, but the lower row corresponds to situation in semi-transparent melt with absorption coefficient 70 m^{-1} . Radiation heat transfer has weakly influenced qualitative distribution of temperature and the location of the hottest melt. Significant changes have been made to the temperature range and the maximal temperature in the melt. Tab. 1. shows integral parameters characterizing the system in superposition of heat exchange processes. For example, in case temperature distributions in opaque or transparent quasi-solid glass and opaque buoyancy driven melt are compared (with other conditions remaining the same) then the range of temperature is diminished from 403 to 116 due to semi-transparency of the quasi-solid melt as well as it is diminished to 139 K in case of opaque buoyancy driven melt. In case all heat transfer mechanisms take place – in EM stirred semi-transparent media homogeneity of temperature due to combination of all processes is much higher – 65 K. Impact of absorption coefficient on volume average temperatures is much lower – variations in volume average temperatures among situations do not exceed 20 K (except the case with quasi-solid opaque glass).

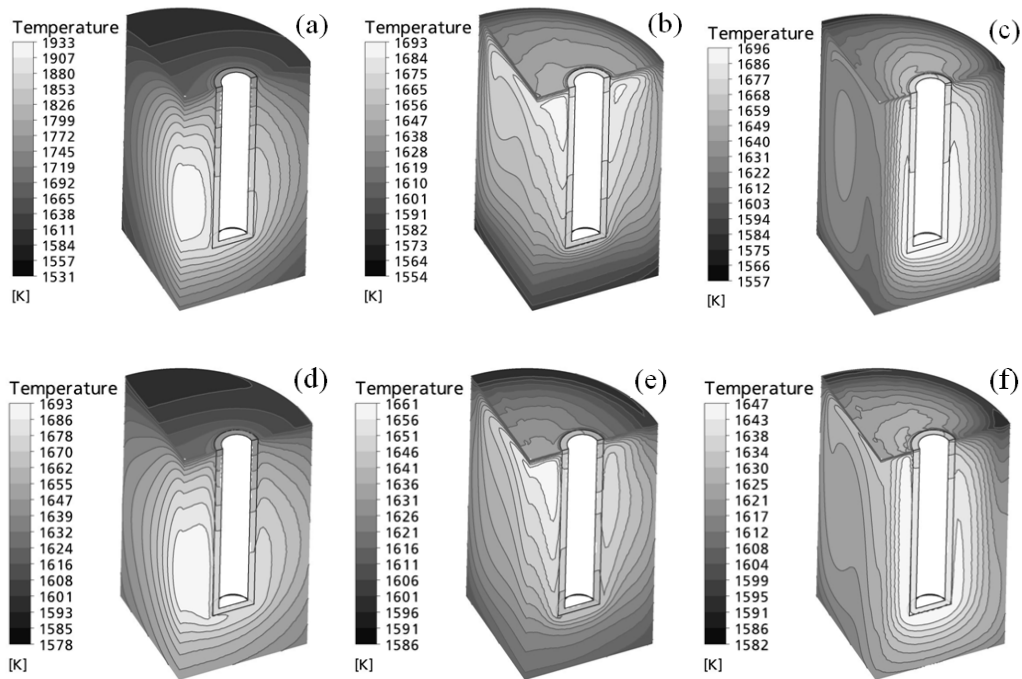


Fig. 4. Temperature distribution: a) conduction, b) conduction and thermal convection, c) conduction, thermal and EM convection, d) conduction and thermal radiation, e) conduction, thermal convection and radiation, f) convection, thermal and EM convection and thermal radiation ($U_{\text{eff}}=20 \text{ V}$, $\alpha=100 \text{ W/m}^2\cdot\text{K}$, $T_s=1500 \text{ K}$)

Tab. 1. Integral parameters of the melt in case of superposition of different heat exchange processes

	v_{max} cm/s	T_{min} K	T_{max} K	ΔT , K	T_{ave} , K
conduction	0.0	1531	1933	403	1714
conduction, radiation	0.0	1578	1693	116	1644
conduction, TC	0.2	1554	1693	139	1634
conduction, TC, EC	2.4	1557	1696	139	1633
conduction, TC, radiation	0.3	1586	1661	75	1628
conduction, TC, EC, radiation	2.5	1582	1647	65	1625

Fig. 5 shows dependence of the temperature range and the maximal temperature in the melt on absorption coefficient. DT, P1 and Rosseland radiation models have been used to obtain it taking into account the usability range [3] of each model.

Correspondence between the results achieved by different methods in case of overlapping absorption is not perfect. Meaning of Fig. 5bd is similar to that of Fig. 3b ($B=0$), except constant physical properties used in Fig. 5. In case of buoyancy driven glass melt the minimum is not as significant as in quasi-solid semi-transparent glass. The most significant increase in both: T_{\max} and ΔT is expected in case absorption approaches optically dense limit.

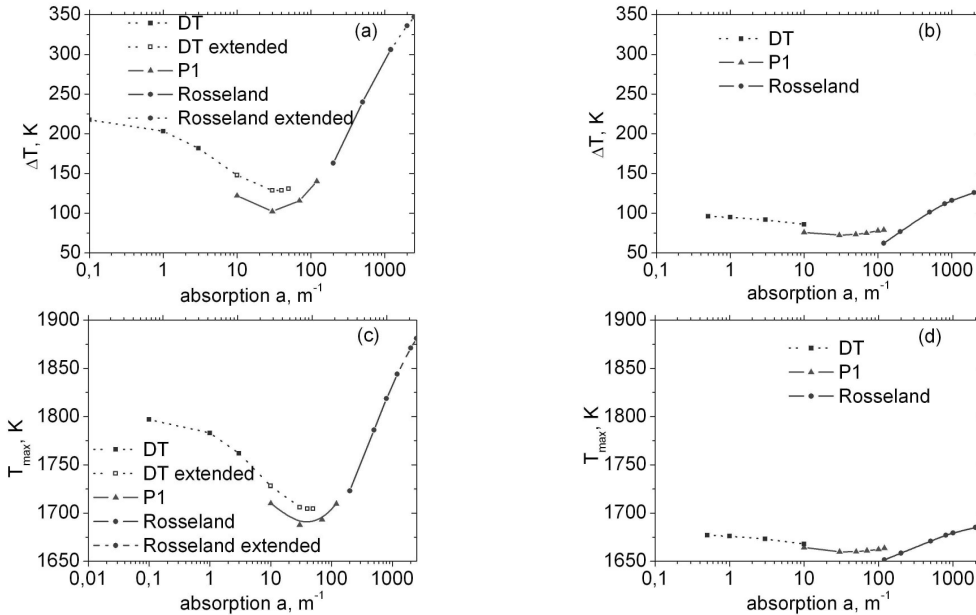


Fig. 5. Dependencies of temperature range (a, b) and the maximal temperature (c, d) on absorption coefficient of the melt: (a, c) quasi-solid semi-transparent melt; (b, d) buoyancy driven semi-transparent melt ($U_{\text{eff}}=20$ V, $\alpha=100$ W/m²·K, $T_s=1500$ K)

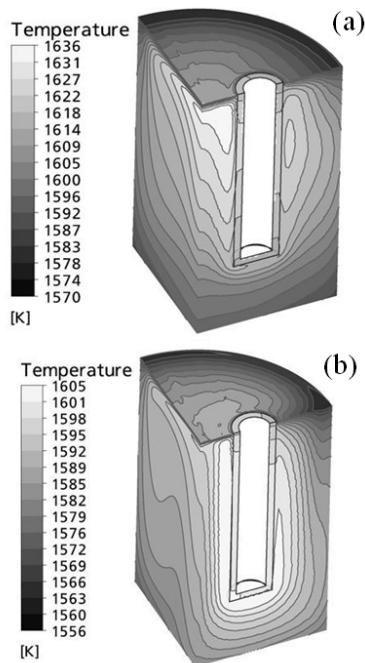


Fig. 6. Temperature distribution: (a) conduction, thermal convection and radiation, (b) conduction, thermal and EM convection and radiation ($U_{\text{eff}}=20$ V, $\alpha=100$ W/m²·K, $T_s=1500$ K)

Fig. 6 shows that only in semi-transparent buoyancy driven melt and semi-transparent buoyancy and EM driven melt temperature distribution results to steady state in case of transient simulation. In other cases overheating occurs.

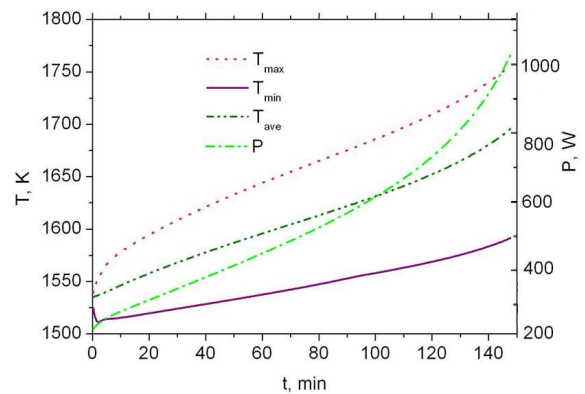


Fig. 7. Transient changes of parameters of the system: the minimum, maximal and volume average temperature and Joule heat production rate in case of thermally and EM driven opaque melt ($U_{\text{eff}}=20$ V, $\alpha=100$ W/m²·K, $T_s=1500$ K)

Tab. 2. Integral parameters of the melt due to interaction of multiple physical processes (temperature dependent physical properties)

	v_{\max} , cm/s	T_{\min} , K	T_{\max} , K	ΔT , K
conduction, TC, radiation	0.3	1570	1636	66
conduction, TC, EC, radiation	1.6	1556	1605	48

case of semi-transparent melt is shown in Fig. 6a. Tab. 2. shows characteristic parameters of the temperature and velocity distribution in case of melt with temperature dependent properties. It shows that resulting state of the real temperature dependent system is more sensitive to influence of radiation heat exchange than the melt with constant physical properties.

Conclusions

Impacts of different heat exchange processes have been extracted from superposition of processes in case of constant physical properties of the melt. Significant influence of radiation heat transfer and thermal convection on stabilisation of temperature distribution has been shown in case of melt with temperature dependent physical properties.

Intuitively expected increase of the maximal temperature and temperature range in the melt in case of increasing optical density (in optically thick absorption range) has been proven for the melt with the constant physical properties.

It has been shown that the maximal temperature and temperature range in the melt in modelled system increases when optical density decreases (in optically thin absorption range) and it arises from radiation heat transfer in the melt. The most significant effect of radiation can be seen in quasi-solid glass.

References

- [1] Cepīte, D., Jakovičs, A., Halbedel, B., Krieger, U.: *Modelling of EM glass convection*. COMPEL Vol. 27 No. 2, 2008, pp. 387-398.
- [2] Jakovičs, A., Cepīte, D., Halbedel, B.: Krieger U.: *Modelling the electromagnetically - driven stirring process of glass melt*. Induktive Verfahren und elektromagnetische Schmelzenbeeinflussung, Ilmenau, 2007, pp. 13.1. – 13.8.
- [3] Versteeg, H., Malalasekera, W.: *An Introduction to Computational Fluid Dynamics: The Finite Volume Method (2nd Edition)*, Prentice Hall, 2007, 520 pp.
- [4] Cepīte, D., Jakovičs, A., Halbedel, B.: *Modelling the temperature homogeneity of the glass melt obtained by EM action*, Proceedings of XXIV UIE International Congress Electricity applications in modern world, Krakow, 2008 (CD)

Authors

Cepite, Daiga
 Prof. Dr.-Phys. Jakovics, Andris
 Faculty of Physics and Mathematics
 University of Latvia
 Zellu str. 8
 LV-1002 Riga, Latvia
 E-mail: daiga.cepite@lu.lv

Prof. Dr.-Ing. Halbedel, Bernd
 Faculty of Mechanical Engineering
 Technical University Ilmenau
 Gustav-Kirchhof Strasse 6
 D-98684, Ilmenau, GERMANY
 E-mail: bernd.halbedel@tu-ilmenau.de